Microchimica Acta (2022) 189: 121
https://doi.org/10.1007/s00604-022-05231-7

ORIGINAL PAPER

Voltammetric picomolar determination of mercury, copper and cadmium using modified pencil graphite electrode with poly-L-cysteine and Fe_3O_4 nanoparticles

Abbas Hassan Oghli[1] · **Ahmad Soleymanpour**[1]

Received: 13 October 2021 / Accepted: 15 February 2022 / Published online: 26 February 2022

Abstract
Cost-effective simultaneous determination of mercury, copper and cadmium ions was performed by differential pulse anodic stripping voltammetry (DPASV) using a pencil graphite electrode (PGE) modified with poly-L-cysteine (P-L-Cys) and Fe_3O_4 nanoparticles. Electropolymerization of L-cysteine was performed by cyclic voltammetry (CV) through applying different cycles. Also, Fe_3O_4 was deposited in a single step by applying a constant potential on the electrode surface in the presence of ferric nitrate. To enhance the sensitivity of measurement, several parameters such as monomer concentration, scan rate, number of cycles in electropolymerization, ferric nitrate concentration, Fe_3O_4 electrodeposition potential and time, and pH of the sample solution were optimized. The surface morphology of the modified electrode was examined by SEM and FTIR. Electrochemical impedance spectroscopy was conducted to investigate the impedance of the electrode surface. The linear ranges for cadmium, copper and mercury were 0.001−2500, 0.0002−3600 and 0.0001−2500 nM with detection limits of 6.4×10^{-13}, 1.0×10^{-13} and 9.0×10^{-14} M, respectively. The stability and reproducibility of the electrode were investigated. Finally, the modified electrode was applied to determine mercury, copper and cadmium in real samples such as the groundwater, Caspian Sea and Tajan River water.

Keywords Modified electrode · Differential pulse voltammetry · Fe_3O_4 nanoparticles · Mercury · Copper · Cadmium

Introduction

Exposure of humans to heavy metals (HMs) has significantly increased [1] because of environmental pollution due to the human activities in mining, smelting industries, home usages and agriculture [2–4]. Pollution by HMs can also occur through the metal corrosion, metal ion erosion, leaching of HMs from the soil, sediment reduction, and volcanic eruption [5]. Heavy metals react with cellular components and cause DNA structural changes that lead to carcinogenesis or apoptosis [6–8]. Several reports have shown that metals such as cadmium [9] and mercury [10] with high toxicity are extremely susceptible reactive oxygen species (ROS), which can eventually lead to cancer [11]. Simultaneous exposure to heavy metals may produce a toxic effect that is more severe and has synergistic destructive effects [11, 12]. Thus, simultaneous measurement of heavy metals with high accuracy, speed and ease plays a significant role in analyzing toxic and hazardous materials.

Various methods for simultaneous measurement of cadmium, copper and mercury have been reported, including electrothermal atomic absorption spectrometry (ETAAS) [13], inductively coupled plasma optical emission spectrometry (ICP-OES) [14–17], inductively coupled plasma-mass spectrometry (ICP-MS) [18–20], atomic absorption spectroscopy [21] and electrochemical methods [22–27]. The electrochemical methods are easy, fast, efficient and low cost [28]. By choosing a working electrode such as pencil graphite, significant advantages including availability, cheapness, high mechanical stability, low residual current, wide potential window, ease of modification and high conductivity can be achieved [29, 30]. The electrochemical methods can be used by portable and on-site measuring devices as inexpensive instruments. In addition to these advantages, the electrochemical sensors are capable to do several measurements simultaneously with one electrode

✉ Ahmad Soleymanpour
soleymanpour@du.ac.ir

[1] School of Chemistry, Damghan University, 3671641167 Damghan, Iran

and cover a wide range of determinations, especially at low concentrations (picomolar to micromolar) [31, 32]. These unique advantages may not be present in other analytical techniques at the same time.

One of the efficient ways to modify the electrode surface is the use of conductive polymers along with nanoparticles [33, 34]. Poly-L-cysteine is one of the conductive polymers that has been used for the modification of electrode surface in various electrochemical configurations for the detection of ions [35–38] and biological compounds [39–47]. P-L-Cys layer coated on the electrode surface increases the target peak current compared to the bare electrode, which has usually been attributed to the microstructure of P-L-Cys [41–44]. A higher increase in signal intensity has been achieved by the combining of metal nanoparticles and P-L-Cys film [33]. Metal nanoparticles such as gold and silver can be easily deposited by covalent bonding to P-L-Cys layers [33, 34]. Carbon-based electrodes are very suitable for electropolymerization by immersing the electrode in a solution of L-cysteine monomer and applying repeated cycles. L-cysteine is oxidized, and cationic amine radicals are produced that react with aromatic carbon on the surface of the electrode and form a carbon–nitrogen bond [42]. The hypersensitivity in electrodes modified with P-L-Cys is unique because it contains an active thiol group that can generate thiol radicals like amino radicals and form bonds with aromatic groups [43]. Since the electron-rich amino group is electroactive at lower potentials than the thiol group, the electrical oxidation deposition of thiols usually requires the presence of strong proton depletion agents [43]. Thus, P-L-Cys can act as a metal chelating agent through the interaction with the thiol groups by applying the appropriate potential [48]. As a family of Lewis soft bases, sulfur-containing species have a highly polarizable donor center that can react strongly with the orbitals of soft Lewis acids such as heavy metal ions [49]. Such chelation between mercury and P-L-Cys has been studied that indicates the high capacity of mercury to form a P-L-Cys-mercury bond. It was shown that the bond formation of mercury is higher than the other metals ions such as Pb(II), Zn(II) and Co(II) [49, 50]. Another study showed that the cadmium and copper binding capacity was higher than the other heavy metals with the sequence of $Cu^{2+} > Cd^{2+} > Ni^{2+} > Pb^{2+} > Co^{2+}$ [48]. Thus, it can be concluded that P-L-Cys has a great tendency to form bonds with heavy metals, and among heavy metals, the binding capacity and priority for copper, cadmium and mercury metals are higher [48–50].

In the electrode modification processes, an iron oxide film as an outer layer of the electrode modified with a polymer can also be used owing to its catalytic properties, cost-effectiveness, good electrical and magnetic properties, and being environmentally friendly [44, 45]. Based on these advantages, magnetite (Fe_3O_4) has been used in various fields such as batteries, sensors, targeted drugs, catalysts, data storage and removal of metal ions from effluents due to its distinctive properties [46, 47]. Various methods have been reported for the fabrication of Fe_3O_4 thin films including pulsed laser deposition (PLD), molecular beam epitaxy (MBE), chemical vapor deposition (CVD) and dispersion techniques, which usually require expensive equipment and relatively alarming test conditions such as high temperature and vacuum control. However, the electrodeposition method is more interested in specific features such as low cost, low temperature and obtaining high-quality Fe_3O_4 thin films [51, 52]. The porous structure of the carbon-base electrode facilitates the diffusion of liquids into the electrode substrate. So, the advantages of mechanical flexibility and high electrical conductivity of the electrode can be accessed, which significantly improve the properties of modification film [53].

In this paper, the voltammetry technique was used to measure cadmium, copper and mercury heavy metals simultaneously. Pencil graphite electrode, an inexpensive carbon-base electrode with a quick and easy modification process, was used as a working electrode. P-L-Cys and Fe_3O_4 were used to modify the electrode by an easy, fast, single-step and in situ electrochemical method. The obtained detection limits revealed that the modified PGE has a very low detection limit and high selectivity, which allow trace analysis of the ions simultaneously in real samples such as the groundwater, Caspian Sea and Tajan River water. The lower detection limit compared to the other electrochemical reports for simultaneous analysis of these three metals, high selectivity, application of cheap PGE as working electrode, ease of modification and ability for precise analysis of the ions in real samples were considered the novelty of the represented electrochemical sensor.

Experimental

Materials and reagents

All materials were provided as analytical grade and used without re-purification. Pencil graphite leads were supplied from a supermarket. Deionized water was utilized for the preparation of all solutions. All chemical salts and solvents were purchased from Merck. Stock solutions of 0.1 M of each three heavy metal ions ($Cd(NO_3)_2$, $Cu(NO_3)_2$ and $HgCl_2$) were provided by the dissolution of appropriate amounts of corresponding salts in 10 mL deionized water. Phosphate buffer solution (PBS, 0.1 M and pH = 7.0) was prepared by the mixing appropriate concentrations of potassium dihydrogen phosphate and phosphoric acid.

Apparatus

Electrochemical analysis was performed by a Potentiostat–Galvanostat Autolab PGSTAT 30 equipped with a three-electrode system using Nova 2.1 software. A 0.9-mm-diameter rotating (Rotring Co. Ltd, Germany, R505210N) pencil lead (type H) with a geometric area of 0.23 cm^2 was applied as a working electrode. A platinum rod and a Metrohm Ag/AgCl (KCl, sat,d) were used as auxiliary and reference electrodes, respectively. Perkin-Elmer RXI FT-IR spectrometer was used for IR spectra. X-ray diffraction (XRD) spectra were obtained with a D8 Advance Bruker diffractometer using CuKα radiation (λ = 0.1540 nm). A Metrohm 827 pH meter was used to adjust the pH of the solutions. SEM spectra were taken by a Leo 1450VP microscope.

Electrode modification with P-L-Cys

P-L-Cys was polymerized by cyclic voltammetry on the surface of the PGE [34]. One end of the PGE was connected to the potentiostat with a copper wire as the working electrode. The other end of the PGE was vertically inserted in a phosphate buffer solution (0.1 M and pH = 7.0) containing L-Cys monomer (5 mM). The cyclic voltammograms were obtained at the PGE surface in the potential range of -1.0 to 2.0 V with a scan rate of 100 mVs^{-1} during five cycles. Finally, a thin layer of P-L-Cys was deposited on the electrode surface during the recording of cyclic voltammograms and then dried slowly at room temperature.

Modification of the electrode with Fe_3O_4

To prepare the iron oxide thin layer, a mixture of 0.8 mM $Fe(NO_3)_3.9H_2O$ in DMSO was sonicated for 10 min. The PGE modified with P-L-Cys (P-L-Cys/PGE) was inserted into the mixture, and then a constant potential of −1.7 V was applied to the electrode for 300 s, which finally led to the construction of Fe_3O_4/P-L-Cys/PGE-modified electrode.

Electrochemical experimental design

A solution containing PBS and analytes of Cd^{2+}, Cu^{2+} and Hg^{2+} was added to the electrochemical cell. The modified PGE was applied as the working electrode. The desired voltammograms were recorded using the DPASV technique by the scanning potential between −0.85 to 0.5 V with adsorption potential of −1.0 V for 15 s. All of the reported results were the average of three repetitive measurements.

Determination of metals ions in real samples

To measure Cd^{2+}, Cu^{2+} and Hg^{2+} in real samples, water of the southern shores of the Caspian Sea (pH = 8.3, EC = 18.5 mS/cm) and Tajan River (pH = 7.4, EC = 415 µS/cm), Sari, Iran was used. Sampling was done from two different places of the river and also seawater inside a one-liter container. After mixing the samples, the filtration was done using Whatman filter paper grade 42. To a 10-mL volumetric flask containing 2 mL of real sample, 4 mL PBS (0.2 M, pH = 3.5) and unknown concentration of Cd^{2+}, Cu^{2+} and Hg^{2+}analytes, different volume of 0.5 µM analytes standard solution (0.1, 0.2, 0.4, 0.7 and 1 mL) were added and filled to the mark with deionized water. The flask content was transferred to the electrochemical cell, and the modified PGE was applied as the working electrode. The desired DPASV voltammograms were recorded after each addition by applying a -1.00 V adsorption potential for 50 s in the potential scan range between -0.85 and 0.40 V (*vs.* Ag/AgCl) with a scan rate of 33 mV/s, step potential of 5 mV. The peak currents were estimated at -0.75, -0.1 and 0.27 V (*vs.* Ag/AgCl) for Cd^{2+}, Cu^{2+} and Hg^{2+}, respectively. Finally, the unknown concentrations of the analytes in the real sample were determined by the standard addition method. This process was repeated three times for each unknown concentration, and the calculated mean value was reported.

Results and discussion

Morphology of the modified electrode surface

The bare PGE was modified by two layers of P-L-Cys and Fe_3O_4 to increase the sensitivity and detection performance of the analytes. These layers improve the effective surface, which increases the determination quality of the analytes. SEM imaging and FTIR spectroscopy were used to investigate the surface modifications. Figure 1 shows the SEM images of the bare and modified electrodes. Figure 1a displays the bare surface of the PGE, which is almost flat. Figure 1b and 1c indicates the surface of the PGE after covering by P-L-Cys. As expected, a layer of polymer without pores uniformly distributed on the surface of the electrode [54], indicating the electropolymerization of L-Cys is performed correctly on the surface of the bare electrode. In Fig. 1d, Fe_3O_4 in the form of fine spherical grains disperses on the surface of the electrode modified with P-L-Cys. Observation of the image quietly confirms the existence of different layers on the electrode in various steps of the electrode modification. The presence of such modifier layers increases the effective surface of the modified electrode.

FT-IR analysis was applied to evaluate the iron oxide layer further. According to the corresponding spectrum in Fig. 2a, the observed band in the region of 595 cm^{-1} belongs to the stretching vibrational mode of oxygen-metal bonds [55, 56], which is attributed to the Fe–O bond in the Fe_3O_4 crystal lattice. Also, the presence of two bands at

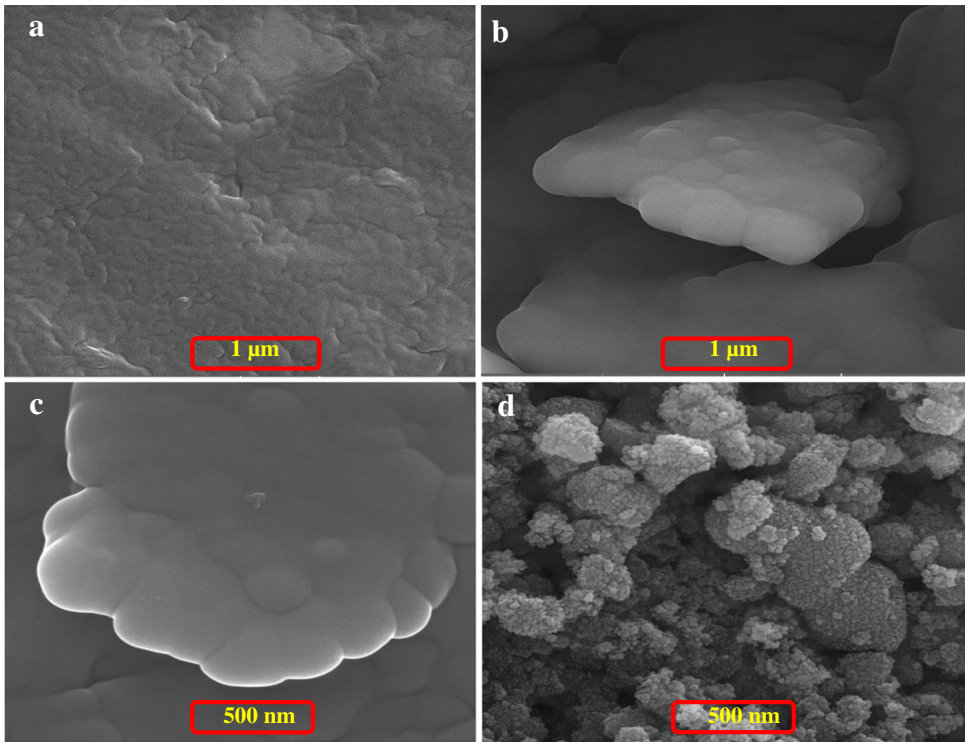

Fig. 1 SEM imaging of the (a) bare PGE, (b) and (c) P-L-Cys/PGE (different magnifications), and (d) Fe_3O_4/P-L-Cys/PGE

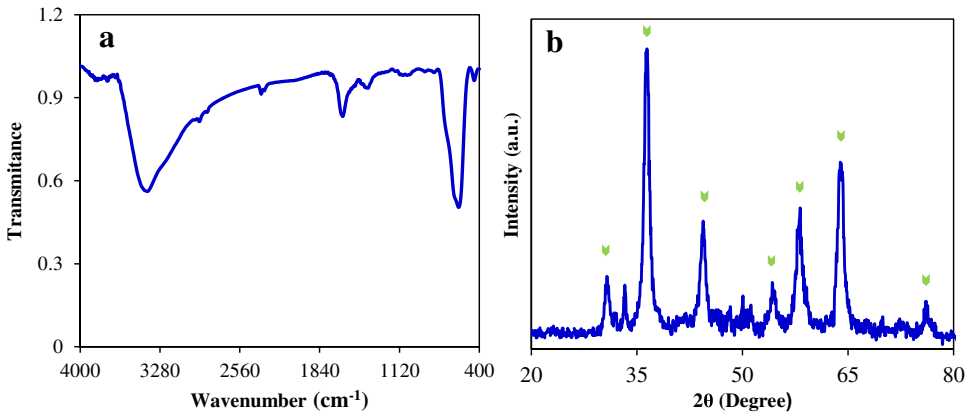

Fig. 2 The FT-IR (a) and XRD (b) spectra of the electrochemically deposited iron oxide on the electrode surface

1640 and 3435 cm^{-1} is related to the presence of hydroxyl groups and attributed to the OH bending and stretching vibrational modes, respectively [57]. X-ray diffraction spectroscopy was also used to investigate the formation of the nanoparticles on the electrode surface (Fig. 2b). The peaks marked in this spectrum correspond to the composition of Fe_3O_4 [58]. According to the spectrum of the nanoparticles and comparison with the other iron oxide compounds [58], it is confirmed that Fe_3O_4 is the dominant compound formed on the electrode surface during the electrochemical deposition. The electrochemical deposition of iron oxide layer can be represented according to the following equation reported by Serrano et al. [59].

$$3Fe^{3+} + 2NO_3^- + 2H_2O + 9e^- \rightarrow Fe_3O_4 + 2NO_2^- + 2H_2$$

Electrochemical characterization of the modified electrode

Electrochemical impedance spectroscopy (EIS) can interpret the changes made on the electrode surface during the electrode modification processes. Figure 3A shows the Nyquist diagram for the bare PGE, P-L-Cys/PGE and Fe_3O_4/P-L-Cys/PGE in the solution containing 0.5 mM $Fe(CN)_6^{-3/-4}$ and 0.1 M KCl. According to curve a, for the bare PGE, the highest value of charge transfer resistance

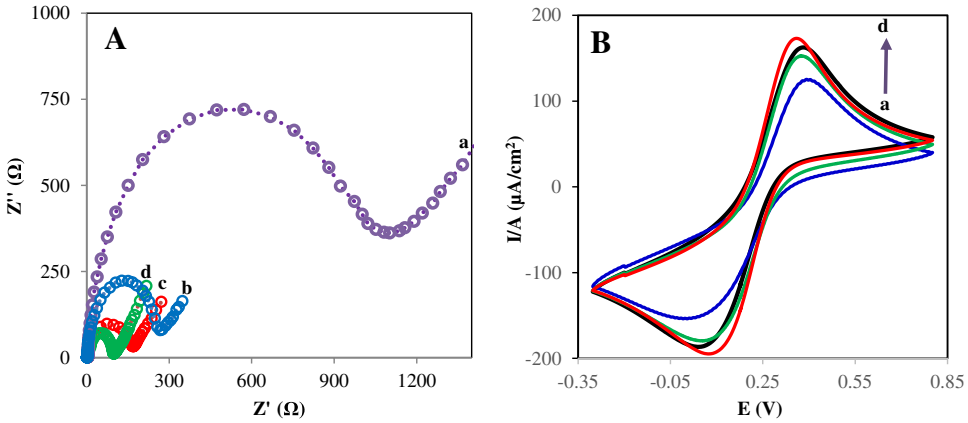

Fig. 3 (A) Nyquist diagrams of (a) bare PGE (b) P-L-Cys/PGE, (c) Fe_3O_4/PGE and (d) Fe_3O_4/P-L-Cys /PGE in $Fe(CN)_6^{-3/-4}$ 5.0 mM and 0.1 M KCl, and (B) cyclic voltammogram of (a) bare PGE (b) P-L-Cys/PGE, (c) Fe_3O_4/PGE and (d) Fe_3O_4/P-L-Cys /PGE in the solution containing $K_3Fe(CN)_6$ 1.0 mM in the presence of KNO_3 0.1 M at scan rates of 100 mV s^{-1}

is observed (R_{ct} = 1200 Ω). Curves b and c show the electrodes modified with P-L-Cys and Fe_3O_4. It can be figured out that the R_{ct} has significantly decreased to 243 and 146 Ω by modifying the electrode with P-L-Cys and Fe_3O_4, respectively. Finally, curve d corresponds to the electrode modified by Fe_3O_4/P-L-Cys, with the lowest R_{ct} (78 Ω). These results clearly confirm the correct process of electrode modification with different layers, which can be due to the appropriate improvement of the electrical properties of the electrode by the deposited P-L-Cys and Fe_3O_4 layers on the electrode surface, as well as the increase of effective surface area and also the electroactive sites. Since both iron oxide and P-L-Cys are conductive materials, their deposition on the electrode surface improves the electrical properties of the electrode and reduces the charge transfer resistance. Cyclic voltammetry technique was also used to support the data obtained by EIS. Figure 3B shows the cyclic voltammograms of $K_3Fe(CN)_6$ 1.0 mM in the presence of KNO_3 0.1 M on the bare and modified PGE electrodes based on the current density. Increasing the current density on the modified electrodes relative to the bare electrode can be a good complement for the impedance results.

To evaluate the effective surface area (A_{eff}) of the bare and modified electrodes, the cyclic voltammograms of 1.0 mM $K_3Fe(CN)_6$ solution containing 0.1 M KNO_3 on the bare and modified electrodes at different scan rates were obtained. Then, the Randles–Sevcik equation at 25 °C was used to calculate the A_{eff} [29].

$$I_p = 2.69 \times 10^5 AD^{1/2} n^{3/2} \nu^{1/2} C$$

where the unit of I_p (peak current value), C (concentration), A (the electrode surface), D (diffusion coefficient, 5.5×10^{-6}) and ν (scan rate) is Ampere, mol/cm^3, cm^2, cm^2/s and v/s, respectively, and n is the number of electrons exchanged in the redox reaction (n = 1). Figure 4 shows the voltammograms for the modified electrode. Using the obtained results and according to the Randles–Sevcik equation, A_{eff}

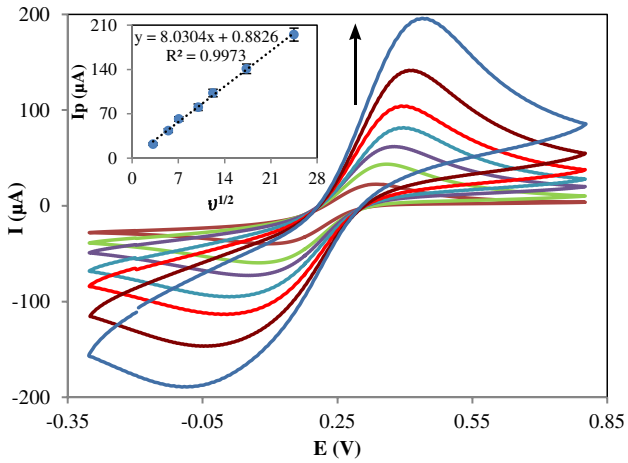

Fig. 4 Cyclic voltammogram of the Fe_3O_4/P-L-Cys /PGE-modified electrode in the solution containing $K_3Fe(CN)_6$ 1.0 mM and KNO_3 0.1 M at the scan rates of 10, 30, 50, 100, 150, 300 and 600 mV s^{-1}. Inset: plot of peak current *vs.* square root of the scan rate

for the bare and final modified electrode (Fe_3O_4/P-L-Cys/PGE) was obtained 0.12 cm^2 and is 0.47 cm^2, respectively, which indicates an increase in the effective surface of the modified electrode. In general, with the information obtained in this section, it can be concluded that the simultaneous increase in conductivity and effective surface have increased the peak currents for measuring the analytes in the modified electrodes.

Electrochemical responses of the modified electrode to heavy metal ions

The response of bare and the modified PGE in a solution containing three heavy metal ions Cu^{2+}, Hg^{2+} and Cd^{2+} were studied to investigate the suitability of the corresponding modified electrode for their determination. Figure 5 shows the DPASV voltammograms of 0.1 nM concentration of

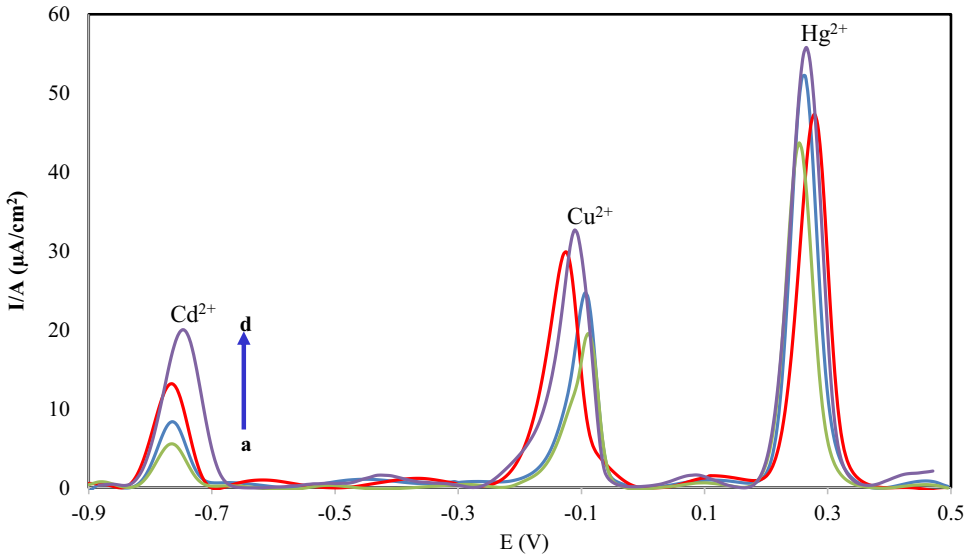

Fig. 5 DPASV voltammograms of Cd^{2+} (0.8 nM), Cu^{2+} (0.1 nM) and Hg^{2+} (0.1 nM) in PBS (pH = 7.0) for (a) bare PGE, (b) P-L-Cys/PGE, (c) Fe_3O_4/PGE and (d) P-L-Cys/Fe_3O_4/PGE

Cu^{2+}, Hg^{2+} and 0.8 nM Cd^{2+} in PBS (0.04 M, pH = 7.0). The peaks observed in the potential range of −0.7, −0.1 and 0.3 V are related to Cd^{2+}, Cu^{2+} and Hg^{2+}, respectively. Among the identified voltammograms, the lowest peak current intensity is related to the bare PGE (a). Voltammogram b is related to the PGE modified with P-L-Cys, and voltammogram c is related to the electrode modification with Fe_3O_4. According to the observed voltammograms, both modifications by P-L-Cys and Fe_3O_4 have increased the peak intensity for all three metal ions. However, the highest peak intensity for the three analytes is related to the electrode modified with two layers of P-L-Cys and Fe_3O_4, which can be related to improving the electrical property of the electrode surface and increasing the effective surface of the electrode by these layers. This confirms the electrode modification has been considerably performed by these two modifier layers.

Optimization of performance factors

The effect of various factors such as monomer concentration, electropolymerization scan rate, number of cycles in the electropolymerization, the iron(III) nitrate concentration, the potential of Fe_3O_4 electrodeposition, applied potential duration time, electrolyte concentration and pH, adsorption potential and its duration time were investigated to obtain the optimal conditions for determination process. Each measurement was repeated three times, and the mean values along with the corresponding error bars were represented as graphs for the concentrations of 0.2 nM of Cu^{2+} and Hg^{2+} and 0.8 nM of Cd^{2+} (Fig. S1). First, the effects of electropolymerization conditions (monomer concentration, electropolymerization scan rate, number of cycles) were investigated. The monomer concentrations of 0.001 to 0.04 M, the sweep rate of 10 to 200 mV/s, and the number of cycles from 1 to 15 in electropolymerization were tested. Their effects on the voltammograms peak current of the analytes are shown in Fig. S1a to S1c. It was concluded that 0.01 M concentration of L-cysteine monomer and five cycles electropolymerization with a scan rate of 100 mV s^{-1} represented the highest electrode response. Next, the conditions corresponding to the Fe_3O_4 electrodeposition on the electrode surface were investigated. Therefore, the concentration of iron(III) nitrate for Fe_3O_4 electrodeposition in the range of 0.1 to 1.2 mM, Fe_3O_4 electrodeposition potential between -0.8 to—1.7 V and potential application time of 10 to 600 s were examined. The results are displayed in Fig. S1d to f. Iron nitrate 0.4 mM with an applied potential of -1.5 V for 200 s was obtained the optimum conditions. Then, the supporting electrolyte (PBS) conditions were investigated, and pH of 3.5 with a concentration of 0.08 M was chosen as the best values (Figs S1g and S1h). Finally, the adsorption potential and its duration time were evaluated. The optimum adsorption potential and time of -1.0 V and 50 s (Figs S1i and S1j) were obtained as the most appropriate values, respectively. Thus, under these definite conditions, the thickness of modifier layers was maintained constant in all subsequent experiments.

Calibration curve and analytical performances

The modified electrode represented well-defined, sharp and separated peaks for the three ions Cd^{2+}, Cu^{2+} and Hg^{2+} which enable simultaneous determination of these ions. The analytical features were determined through the resulting calibration curve for different concentrations of the analytes using the modified electrode under optimal conditions. Figure 6 shows the voltammograms and corresponding calibration curves for different concentrations of Cd^{2+}, Cu^{2+}

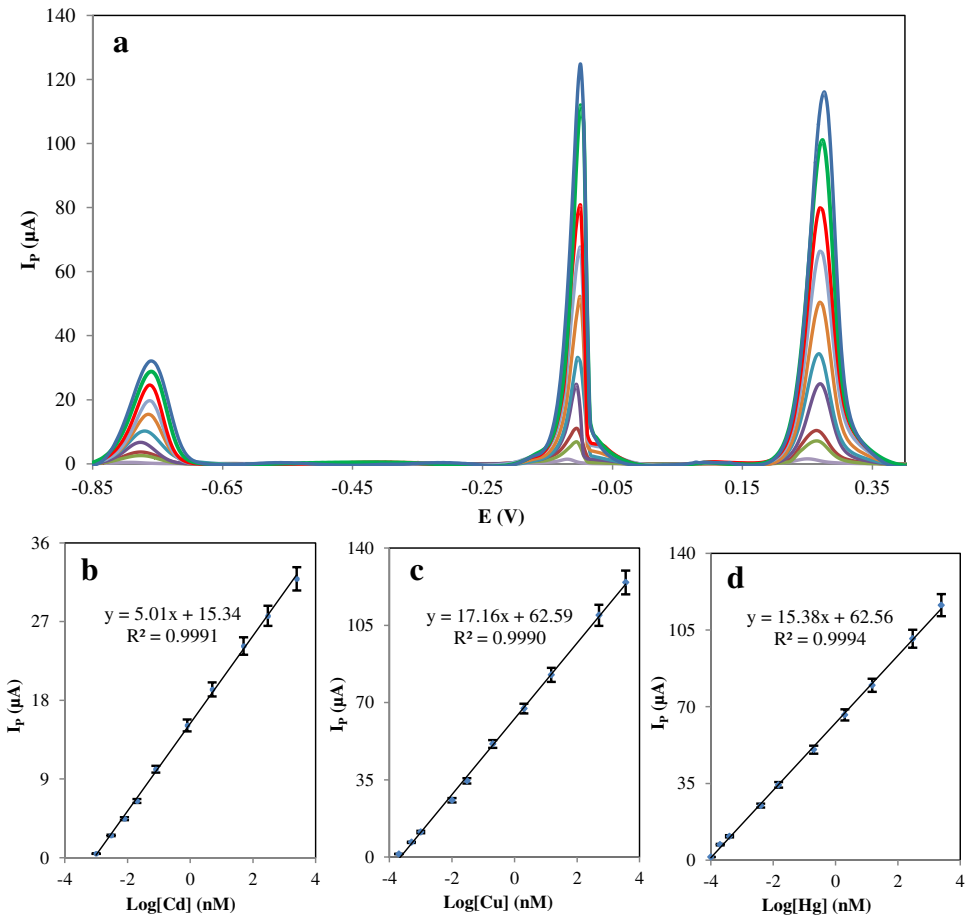

Fig. 6 (a) DPASV voltammograms for Cd^{2+} (0.001−2500 nM), Cu^{2+} (0.002−3600 nM) and Hg^{2+} (0.0001–2500 nM) in PBS (pH = 3.5) on the modified electrode by applying a -1.00 V adsorption potential for 50 s in the potential scan range of -0.85 and 0.40 V (vs. Ag/AgCl) with a scan rate of 33 mV/s and step potential of 5 mV. Calibration curves obtained from I_Ps *vs.* analyte concentrations for (b) Cd^{2+}, (c) Cu^{2+} and (d) Hg^{2+}

and Hg^{2+}. According to the obtained calibration curves, the linear ranges of 0.001 to 2500, 0.0002 to 3600 and 0.0001 to 2500 nM were obtained for Cd^{2+}, Cu^{2+} and Hg^{2+}, respectively. The detection limit based on the equation of $3S_b/m$, where S_b was the blank current standard deviation at E_p for 5 replicate blank measurements and m was the slope of calibration graph of each analyte, were obtained 6.4×10^{-13}, 1.0×10^{-13} and 9.0×10^{-14} M for Cd^{2+}, Cu^{2+} and Hg^{2+}, respectively.

The reproducibility, repeatability and stability of the modified electrode were also evaluated. For this purpose, nine electrodes were simultaneously prepared. Using five

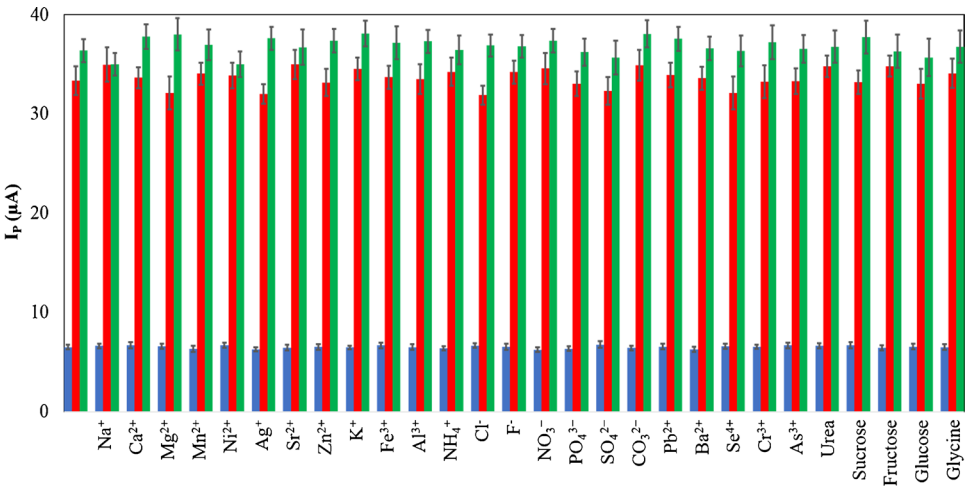

Fig. 7 I_p diagrams of the analytes (0.02 nM) at the presence of various interfering species (the first triple diagram from the left is related to the analytes at the absence of interference, and Cd^{2+}, Cu^{2+} and Hg^{2+})

electrodes, the reproducibility of the modified electrode for 10 nM concentration of the analytes was investigated. According to the I_ps obtained for Cd^{2+}, Cu^{2+} and Hg^{2+}, the RSDs were 3.61%, 3.96% and 3.27%, respectively. Repeatability was also assessed by five replicative measurements of the analytes (10 nM) using one modified electrode. After each measurement, the surface of the electrode was washed with an acidic solution and deionized water. The obtained RSDs for Cd^{2+}, Cu^{2+} and Hg^{2+} peak currents were 3.97%, 4.24% and 4.81%, respectively. With the other three electrodes, the stability of the modified electrode was evaluated for 15 days. Therefore, three electrodes were used to obtain the voltammograms of Cd^{2+}, Cu^{2+} and Hg^{2+} (10 nM) on the first, seventh and fifteenth days. Using the obtained peak currents for Cd^{2+}, Cu^{2+} and Hg^{2+}, the RSDs of 3.86%, 3.43% and 3.27% were calculated. These results indicated that the designed modified electrode has good repeatability and stability (valuable analytical factors) for detecting the analytes.

Investigation of chemical interference and electrode selectivity

The effect of chemical species on the signals of the analytes was investigated to figure out the interference of foreign species which may be present in the analytical sample. The basis of the interference is the maximum concentration of the interfering species, which causes an error of less than 5% [60] of the recorded signal for 0.02 nM concentration of each analyte. The obtained responses of the analytes at the presence of different interferent, ionic species such as Na^{+}, Ca^{2+}, Mg^{2+}, Mn^{2+}, Ni^{2+}, Ag^{+}, Sr^{2+}, Zn^{2+}, K^{+}, Al^{3+}, NH_4^{+}, Cl^{-}, F^{-}, NO_3^{-}, PO_4^{3-}, SO_4^{2-}, CO_3^{2-}, Pb^{2+}, Ba^{2+} urea, sucrose, fructose, glucose and glycine up to a concentration ratio of 500, and Fe^{3+}, Se^{+4}, Cr^{+3} and As^{+3} up to a concentration of 100 times didn't have any significant interference. The observed changes for the signal of the three analytes (0.02 nM) at the presence of various interfering species at the tolerance concentration limit are displayed in Fig. 7. The amount of signal changes were in the range of 0.5%–4.9%, indicating the appropriate selectivity of the modified electrode in different chemical environments.

Application of the developed sensor to the analysis of HMs

To evaluate the ability of the sensor to measure Cd^{2+}, Cu^{2+} and Hg^{2+} in real samples, the water of the southern shores of the Caspian Sea, the water of the Tajan River (Sari, Iran) and groundwater (Damghan, Iran) were used. The standard addition method was applied to obtain each initial unknown concentration using five standard concentrations and three repetitions for each determination. The obtained results are

Table 1 Measurement of Cd^{2+}, Cu^{2+} and Hg^{2+} in real water samples

Real Sample	Added (nM)			Found (nM)[a] PGE Sensor			Found (nM)[a] ICP-OES			Recovery (%)			RSD			t-value (4.30)[b]		
	Cd^{2+}	Cu^{2+}	Hg^{2+}	Cd^{2+}	Cu^{2+}	Hg^{2+}	Cd^{2+}	Cu^{2+}	Hg^{2+}	Cd^{2+}	Cu^{2+}	Hg^{2+}	Cd^{2+}	Cu^{2+}	Hg^{2+}	Cd^{2+}	Cu^{2+}	Hg^{2+}
River water	`0.00	0.00	0.00	1.21 ± 0.04	1.97 ± 0.08	1.38 ± 0.05	1.19 ± 0.03	1.95 ± 0.06	1.39 ± 0.05	-	-	-	3.38	4.21	3.86	-	-	-
	1.00	1.00	1.00	2.23 ± 0.09	2.99 ± 0.11	2.35 ± 0.10	2.20 ± 0.08	2.94 ± 0.10	2.37 ± 0.09	102.0	102.0	97.0	4.12	3.78	4.06	0.44	0.31	0.52
	15.00	15.00	15.00	15.88 ± 0.67	17.51 ± 0.70	16.00 ± 0.66	16.01 ± 0.58	16.83 ± 0.61	16.26 ± 0.57	97.8	103.6	97.5	4.21	3.98	4.13	0.85	1.34	1.01
Sea water	0.00	0.00	0.00	1.58 ± 0.06	2.04 ± 0.07	1.69 ± 0.07	1.64 ± 0.06	2.17 ± 0.05	1.72 ± 0.05	-	-	-	4.06	3.29	4.02	-	-	-
	1.00	1.00	1.00	2.61 ± 0.09	3.02 ± 0.13	2.66 ± 0.10	2.69 ± 0.10	3.24 ± 0.12	2.80 ± 0.11	103.0	98.0	97.0	3.49	4.41	3.76	0.58	0.27	0.52
	15.00	15.00	15.00	16.25 ± 0.62	17.33 ± 0.62	17.34 ± 0.71	16.41 ± 0.57	16.63 ± 0.61	16.39 ± 0.77	97.8	101.9	104.3	3.81	3.58	4.11	0.92	0.81	1.59
Ground water	0.00	0.00	0.00	1.61 ± 0.07	1.76 ± 0.08	1.54 ± 0.07	1.73 ± 0.05	2.03 ± 0.06	1.62 ± 0.05	-	-	-	4.35	4.55	4.55	-	-	-
	1.00	1.00	1.00	2.59 ± 0.12	2.8 ± 0.13	2.59 ± 0.11	2.64 ± 0.09	3.01 ± 0.13	2.53 ± 0.10	98.0	104.0	105.0	4.63	4.64	4.25	0.29	0.53	0.79
	15.00	15.00	15.00	16.29 ± 0.69	16.92 ± 0.81	16.08 ± 0.70	16.77 ± 0.51	17.48 ± 0.74	16.06 ± 0.73	97.9	101.0	96.9	4.24	4.79	4.35	0.80	0.34	1.14

[a] Three measurements average

[b] Critical t-value at two degrees of freedom and 95% confidence limit

Table 2 Comparison of designed sensor with the other reported voltammetric sensors for the determination of the analytes

Modifier/electrode	Analyte	Linear range (M)	Detection limit (M)	Ref
(L-MNPs-CPE)[a]	Cd	–	1.8×10^{-9}	[24]
	Cu	–	1.4×10^{-8}	
	Hg	–	5.0×10^{-9}	
(FGP/AuNC/GCE)[b]	Cd	3.5×10^{-8}—5.3×10^{-5}	8.0×10^{-10}	[25]
	Cu	6.3×10^{-8}- 6.3×10^{-5}	2.9×10^{-9}	
	Hg	3.0×10^{-8}- 2.5×10^{-5}	4.9×10^{-11}	
(AFO/GCE)[c]	Cd	1.0×10^{-8}- 1.0×10^{-6}	4.0×10^{-9}	[26]
	Cu	1.0×10^{-8} -1.0×10^{-6}	5.0×10^{-9}	
	Hg	1.0×10^{-8} -1.0×10^{-6}	1.5×10^{-9}	
Stainless steel electrode (Type 304)	Cd	5.0×10^{-7} -5.0×10^{-6}	2.3×10^{-7}	[27]
	Cu	7.5×10^{-8} -5.0×10^{-6}	7.3×10^{-9}	
	Hg	1.0×10^{-7} -5.0×10^{-6}	2.8×10^{-8}	
(rGO/SnO2/PPy/GCE)[d]	Cd	–	7.5×10^{-13}	[22]
	Cu	–	8.3×10^{-13}	
	Hg	–	8.1×10^{-13}	
(CISPE)[e]	Cd	6.0×10^{-7} -3.0×10^{-5}	8.0×10^{-8}	[23]
	Cu	3.0×10^{-7} -1.0×10^{-4}	6.0×10^{-8}	
	Hg	8.0×10^{-8} -5.0×10^{-5}	1.0×10^{-8}	
(L-MSNPs/CPE)[f]	Cd	1.3×10^{-8} -8.9×10^{-6}	2.6×10^{-9}	[61]
	Cu	9.4×10^{-9} -1.7×10^{-5}	1.5×10^{-9}	
	Hg	2.5×10^{-9} -5.0×10^{-6}	2.5×10^{-10}	
P-L-Cys/Fe_3O_4/PGE	Cd	1.0×10^{-12} -2.5×10^{-6}	6.4×10^{-13}	This work
	Cu	5.0×10^{-13} -3.6×10^{-6}	1.0×10^{-13}	
	Hg	1.0×10^{-13} -2.5×10^{-6}	9.0×10^{-14}	

[a] Ligand-coated magnetite nanoparticles carbon paste electrode

[b] Fluorinated graphene/gold nanocage/glassy carbon electrode

[c] Aluminum ferrite/glassy carbon electrode

[d] Reduced graphene oxide/SnO2/polypyrrole/glassy carbon electrode

[e] Ionic liquid-functionalized ordered mesoporous silica SBA-15-modified carbon paste electrode

[f] Ligand-modified silica nanoparticles/carbon paste electrode

represented in Table 1. The achieved results from ICP-OES are also displayed in Table 1. From the data in Table 1, it is clear that the determination results of the sensor were in satisfactory agreement with those obtained by ICP-OES. Moreover, the results obtained for the recoveries and RSDs indicated high ability of the modified electrode to determine Cd^{2+}, Cu^{2+} and Hg^{2+} in the samples.

Comparison of the designed sensor with other reported voltammetric sensors

The modified electrode was compared with the other reported voltammetric sensors for the simultaneous determination of Cd^{2+}, Cu^{2+} and Hg^{2+} (Table 2). According to the data in this table, it can be concluded that the developed modified electrode is superior in terms of diagnostic performances to those previously reported for the simultaneous analysis of these three heavy metals. Furthermore, it is important to note that the sensor was designed using the cheapest electrode (pencil graphite) with an easy and fast modification procedure. These features along with the high selectivity make the sensor an alternative tool for the facile and precise determination of the three significant water pollutants, which is very important for living things.

Conclusion

Simultaneous measurement of HMs containing cadmium, copper and mercury was performed by a modified pencil graphite electrode. The electrode was modified

by a double-layer of poly-L-cysteine and iron oxide, deposited on the electrode surface in a quick and easy electrochemical procedure. Electrode modification by these two layers increased the effective surface area and decreased the charge transfer resistance. As a result of this modification, analytes measurement was performed in a wide range with the lowest detection limit compared to other reported simultaneous measurement methods. The designed sensor was used to measure the metals in real samples (groundwater, Caspian Sea and Tajan River water), which displayed satisfactory results in terms of recovery and accuracy. By comparing the developed sensor with the other electrochemical sensors for the analytes, it was concluded that the sensor has superior linear range and detection limit.

Supplementary Information The online version contains supplementary material available at https://doi.org/10.1007/s00604-022-05231-7.

Acknowledgements We would like to thank Damghan University Research Council for supporting this research.

Declarations

Conflict of interest The authors declare that they have no competing interests.

References

1. Bradl H (2005) Heavy metals in the environment: origin, interaction and remediation. Academic Press, London, Vol, p 6
2. He ZL, Yang XE, Stoffella PJ (2005) Trace elements in agroecosystems and impacts on the environment. J Trace Elem Med Biol 19:125–140
3. Herawati N, Suzuki S, Hayashi K, Rivai IF, Koyoma H (2000) Cadmium, copper and zinc levels in rice and soil of Japan, Indonesia and China by soil type. Bull Environ Contam Toxicol 64:33–39
4. Shallari S, Schwartz C, Hasko A, Morel JL (1998) Heavy metals in soils and plants of serpentine and industrial sites of Albania. Sci Total Environ 209:133–142
5. Nriagu JO (1989) A global assessment of natural sources of atmospheric trace metals. Nature 338:47–49
6. Tchounwou P, Newsome C, Williams J, Glass K (2008) Copper-induced cytotoxicity and transcriptional activation of stress genes in human liver carcinoma (HepG2) cells. Metal Ions Biol Med 10:285–290
7. Wang S, Shi X (2001) Molecular mechanisms of metal toxicity and carcinogenesis. Mol Cell Biochem 222:3–9
8. Beyersmann D, Hartwig A (2008) Carcinogenic metal compounds: recent insight into molecular and cellular mechanisms. Arch Toxicol 82:493–512
9. Tchounwou PB, Ishaque A, Schneider J (2001) Cytotoxicity and transcriptional activation of stress genes in human liver carcinoma cells (HepG2) exposed to cadmium chloride. Mol Cell Biochem 222:21–28
10. Sutton D, Tchounwou PB, Ninashvili N, Shen E (2002) Mercury induces cytotoxicity, and transcriptionally activates stress genes in human liver carcinoma cells. Int J Mol Sci 3:965–984
11. Tchounwou PB, Yedjou CG, Patlolla AK, Sutton DJ (2012) Heavy metal toxicity and the environment. Mol Clin Environ Toxicol 2012:133–164
12. Wang G, Fowler BA (2008) Roles of biomarkers in evaluating interactions among mixtures of lead, cadmium and arsenic. Toxicol Appl Pharmacol 233:92–99
13. Sardans J, Montes F, Peñuelas J (2010) Determination of As, Cd, Cu, Hg and Pb in biological samples by modern electrothermal atomic absorption spectrometry. Spectrochim Acta B 65:97–112
14. Chaves ES, dos Santos EJ, Araujo RG, Oliveira JV, Frescura VLA, Curtius AJ (2010) Metals and phosphorus determination in vegetable seeds used in the production of biodiesel by ICP OES and ICP-MS. Microchem J 96:71–76
15. Llorent-Martinez EJ, De Cordova MF, Ruiz-Medina A, Ortega-Barrales P (2012) Analysis of 20 trace and minor elements in soy and dairy yogurts by ICP-MS. Microchem J 102:23–27
16. Nardi VEP, Evangelista FS, Tormen L, Saint TD, Curtius AJ, de Souza SJ, Barbosa F (2009) The use of inductively coupled plasma mass spectrometry (ICP-MS) for the determination of toxic and essential elements in different types of food samples. Food Chem 112:727–732
17. Wheal MS, Fowles TO, Palmer LT (2011) A cost-effective acid digestion method using closed polypropylene tubes for inductively coupled plasma optical emission spectrometry (ICP-OES) analysis of plant essential elements. Anal Methods 3:2854–2863
18. Tarantino TB, Barbosa IS, Lima DDC, Pereira MDG, Teixeira LS, Korn MGA (2017) Microwave-assisted digestion using diluted nitric acid for multi-element determination in rice by ICP OES and ICP-MS. Food Anal Methods 10:1007–1101
19. Dico GML, Galvano F, Dugo G, D'ascenzi C, Macaluso A, Vella A, Giangrosso G, Cammilleri G, Ferrantelli V (2018) Toxic metal levels in cocoa powder and chocolate by ICP-MS method after microwave-assisted digestion. Food Chem 245:1163–2116
20. Huang C, Hu B (2008) Silica-coated magnetic nanoparticles modified with γ-mercaptopropyltrimethoxysilane for fast and selective solid phase extraction of trace amounts of Cd, Cu, Hg, and Pb in environmental and biological samples prior to their determination by inductively coupled plasma mass spectrometry. Spectrochim Acta B 63:437–444
21. Benes B, Sladka J, Spevackova V, Smid J (2003) Determination of normal concentration levels of Cd, Cr, Cu, Hg, Pb, Se and Zn in hair of the child population in the Czech Republic. Cent Eur J public health 11:184–186
22. Rehman AU, Ikram M, Kan K, Zhao Y, Zhang WJ, Zhang J, Liu Y, Wang Y, Du L, Shi K (2018) 3D interlayer nanohybrids composed of reduced graphenescheme oxide/SnO2/PPy grown from expanded graphite for the detection of ultra-trace Cd^{2+}, Cu^{2+}, Hg^{2+} and Pb^{2+} ions. Sensors Actuators B 274:285–295
23. Zhang P, Dong S, Gu G, Huang T (2010) Simultaneous determination of Cd^{2+}, Pb^{2+}, Cu^{2+} and Hg^{2+} at a carbon paste electrode modified with ionic liquid-functionalized ordered mesoporous silica. Bull Korean Chem Soc 31:2949–2954
24. Afkhami A, Moosavi R, Madrakian T, Keypour H, Ramezani-Aktij A, Mirzaei-Monsef M (2014) Construction and application of an electrochemical sensor for simultaneous determination of Cd (II), Cu (II) and Hg (II) in water and foodstuff samples. Electroanalysis 26:786–795
25. Tan Z, Wu W, Feng C, Wu H, Zhang Z (2020) Simultaneous determination of heavy metals by an electrochemical method based on a nanocomposite consisting of fluorinated graphene and gold nanocage. Microchim Acta 187:1–9
26. Durai L, Badhulika S (2020) Simultaneous sensing of copper, lead, cadmium and mercury traces in human blood serum using orthorhombic phase aluminium ferrite. Mater Sci Eng C 112:110865

27. Kitte SA, Li S, Nsabimana A, Gao W, Lai J, Liu Z, Xu G (2019) Stainless steel electrode for simultaneous stripping analysis of Cd (II), Pb (II), Cu (II) and Hg (II). Talanta 191:485–490
28. Nemiwal M, Kumar D (2021) Recent progress on electrochemical sensing strategies as comprehensive point-care method. Monatsh Chem 152:1–18
29. Hassan Oghli A, Soleymanpour A (2020) Polyoxometalate/reduced graphene oxide modified pencil graphite sensor for the electrochemical trace determination of paroxetine in biological and pharmaceutical media. Mater Sci Eng C 108:110407
30. Hassan Oghli A, Soleymanpour A (2021) Pencil graphite electrode modified with nitrogen-doped graphene and molecular imprinted polyacrylamide/sol-gel as an ultrasensitive electrochemical sensor for the determination of fexofenadine in biological media. Biochem Eng J 167:107920
31. Hasanjani HRA, Zarei K (2019) An electrochemical sensor for attomolar determination of mercury (II) using DNA/poly-L-methionine-gold nanoparticles/pencil graphite electrode. Biosens Bioelectron 128:1–8
32. Taheri M, Ahour F, Keshipour S (2018) Sensitive and selective determination of Cu^{2+} at d-penicillamine functionalized nanocellulose modified pencil graphite electrode. J Phys Chem Solids 117:180–187
33. Dehnavi A, Soleymanpour A (2021) Silver nanoparticles/poly (L-cysteine) nanocomposite modified pencil graphite for selective electrochemical measurement of guaifenesin in real samples. Measurement 175:109103
34. Tıg GA (2017) Highly sensitive amperometric biosensor for determination of NADH and ethanol based on Au-Ag nanoparticles/poly (L-cysteine)/reduced graphene oxide nanocomposite. Talanta 175:382–389
35. Autry HA, Holcombe JA (1995) Cadmium, copper and zinc complexes of poly-L-cysteine. Analyst 120:2643–2648
36. Jurbergs HA, Holcombe JA (1997) Characterization of Immobilized Poly(L-cysteine) for cadmium chelation and preconcentration. Anal Chem 69:1893–1898
37. Howard M, Jurbergs HA, Holcombe JA (1998) Effects of oxidation of immobilized poly(L-cysteine) on trace metal chelation and preconcentration. Anal Chem 70:1604–1609
38. White BR, Stackhouse BT, Holcombe JA (2009) Magnetic γ-Fe_2O_3 nanoparticles coated with poly-l-cysteine for chelation of As(III), Cu(II), Cd(II), Ni(II), Pb(II) and Zn(II). J Hazard Mater 161:848–853
39. Zheng X, Zhou D, Xiang D, Huang W, Lu S (2009) Electrochemical determination of ascorbic acid using the poly-cysteine film-modified electrode. Russ J Electrochem 45:1183–1187
40. Tang Y, Wang Y, Liu G, Sun D (2016) Determination of sunset yellow and tartrazine using silver and poly (L-cysteine) composite film modified glassy carbon electrode. Indian J Chem 55:298–303
41. Gu Y, Liu W, Chen R, Zhang L, Zhang Z (2013) Cyclodextrin-Functionalized gold nanoparticles/poly(L-cysteine) modified glassy carbon electrode for sensitive determination of metronidazole. Electroanalysis 25:1209–1216
42. Deinhammer RS, Ho M, Anderegg JW, Porter MD, Deinhammer RS, Ho M, Anderegg JW (1994) Electrochemical oxidation of amine-containing compounds: A route to the surface modification of glassy carbon electrodes. Langmuir 10:1306–1313
43. Pchelintsev NA, Vakurov A, Hays HH, Millner PA (2011) Thiols deposition onto the surface of glassy carbon electrodes mediated by electrical potential. Electrochim Acta 56:2696–2702
44. He HK, Gao C (2010) Supraparamagnetic, conductive, and processable multifunctional graphene nanosheets coated with highdensity Fe_3O_4 nanoparticles. ACS Appl Mater Interfaces 2:3201–3210
45. Su J, Cao MH, Ren L, Hu CW (2011) Fe_3O_4–graphene nanocomposites with improved lithium storage and magnetism properties. J Phys Chem C 115:14469–14477
46. Liang C, Huang S, Zhao W, Liu W, Chen J, Liu H, Tong Y (2015) Polyhedral Fe_3O_4 nanoparticles for lithium ion storage. New J Chem 39:2651–2656
47. Ngomsik AF, Bee A, Draye M, Cote G, Cabuil V (2005) Magnetic nano-and microparticles for metal removal and environmental applications: a review. CR Chim 8:963–970
48. Johnson AM, Holcombe JA (2005) Poly (L-cysteine) as an electrochemically modifiable ligand for trace metal chelation. Anal chem 77:30–35
49. Zhang HL, Cai H, Xia Y, Zhang P, Xiong SW, Gai JG (2020) An l-cystine/l-cysteine impregnated nanofiltration membrane with the superior performance of an anchoring heavy metal in wastewater. RSC Adv 10:3438–3449
50. Uzun L, Türkmen D, Yılmaz E, Denizli BS, A, (2008) Cysteine functionalized poly (hydroxyethyl methacrylate) monolith for heavy metal removal. Colloid Surf Physicochem Eng Aspects 330:161–167
51. Wang X, Liao Y, Zhang D, Wen T, Zhong Z (2018) A review of Fe_3O_4 thin films: Synthesis, modification and applications. J Mater Sci Technol 34:1259–1272
52. Chung KW, Kim KB, Han S-H, Lee H (2005) Novel synthesis and electrochemical characterization of nano-sized cellular Fe_3O_4 thin film. Electrochem Solid-State Lett 8:A259–A262
53. Li D, Zhou X, Xu Z, Man J, Yuan B, Liu Y, Ortega CM, Sun L, Liu Z (2015) Electrodeposition of micro-nano size Fe_3O_4 crystals anchored on flexible buckypaper. J Solid State Electrochem 19:3053–3058
54. Ulkoski D, Scholz C (2017) Synthesis and application of aurophilic poly (cysteine) and poly (cysteine)-containing copolymers. Polymers 9:500
55. Waldron R (1955) Infrared spectra of ferrites. Phys Rev 99:1727–1735
56. Bordbar AK, Rastegari AA, Amiri R, Ranjbakhsh E, Abbasi M, Khosropour AR (2014) Characterization of Modified Magnetite Nanoparticles for Albumin Immobilization. Biotechnol Res Inter 2014:1–6
57. Nalbandian L, Patrikiadou E, Zaspalis V, Patrikidou A, Hatzidaki E, Papandreou CN (2016) Magnetic nanoparticles in medical diagnostic applications: Synthesis, characterization and proteins conjugation. Curr Nanosci 12:455–468
58. Noval V.E, Carriazo J.G (2019) Fe_3O_4-TiO_2 and Fe_3O_4-SiO_2 core-shell powders synthesized from industrially processed magnetite (Fe_3O_4) microparticles. Mater Res 22
59. Ibrahim M, Serrano KG, Noe L, Garcia C, Verelst M (2009) Electro-precipitation of magnetite nanoparticles: An electrochemical study. Electrochim Acta 55:155–158
60. Rouhani M, Soleymanpour A (2020) Molecularly imprinted sol-gel electrochemical sensor for sildenafil based on a pencil graphite electrode modified by preyssler heteropolyacid/gold nanoparticles/MWCNT nanocomposite. Microchim Acta 187:1–16
61. Afkhami A, Soltani-Felehgari F, Madrakian T, Ghaedi H, Rezaeivala M (2013) Fabrication and application of a new modified electrochemical sensor using nano-silica and a newly synthesized Schiff base for simultaneous determination of Cd^{2+}, Cu^{2+} and Hg^{2+} ions in water and some foodstuff samples. Anal Chim Acta 10:21–30